Infrared spectroscopy of CO_2–D(H)Br: Molecular structure and its reliability

Y. P. Zeng, S. W. Sharpe,[a] S. K. Shin,[b] C. Wittig, and R. A. Beaudet
Department of Chemistry, University of Southern California, Los Angeles, California 90089-0482

(Received 3 May 1992; accepted 23 June 1992)

A high resolution rovibrational absorption spectrum of the weakly bonded CO_2–DBr complex has been recorded in the 2350 cm^{-1} region by exciting the CO_2 asymmetric stretch vibration with a tunable diode laser. The CO_2–DBr band origin associated with this mode is 2348.2710 cm^{-1}, red-shifted by 0.87 cm^{-1} from uncomplexed CO_2. The position of the hydrogen atom is determined from differences in moments-of-inertia between CO_2–DBr and CO_2–HBr, i.e., by using the Kraitchman method. From this, we conclude that ground state CO_2–H(D)Br has an average geometry that is planar and inertially T-shaped, with essentially parallel HBr and CO_2 axes. Average values of intermolecular parameters are: $R_{cm}=3.58$ Å, $\theta_{BrCO}=79.8°$, and $\theta_{HBrC}=93.1°$. The validity of using the Kraitchman method, which was designed for use with rigid molecules, with a floppy complex like CO_2–HBr is discussed. The experimental structure is corroborated qualitatively by results from Møller–Plesset second-order perturbation calculations, corrected for basis set superposition errors. The theoretical equilibrium geometry for the inertially T-shaped complex is planar with structural parameters: $R_{CBr}=3.62$ Å, $\theta_{BrCO}=89°$, and $\theta_{HBrC}=86°$. A number of cuts on the four dimensional intermolecular potential surface confirm large zero-point amplitudes, which are known to be characteristic of such systems, and these cuts are used to estimate tunneling splittings. Tunneling is shown to occur by out-of-plane rotation of the H atom, in accord with the experimental observations of Rice *et al.* There is no significant in-plane tunneling. A quasilinear hingelike isomer (OCO–HBr) with $R_{OH}=2.35$ Å at equilibrium is calculated to be as stable as the T-shaped complex; however, this species has yet to be observed experimentally. Photoinitiated reactions in CO_2–HX complexes are discussed.

I. INTRODUCTION

Weakly bonded binary complexes have been successfully used in studies of elementary chemical reaction dynamics.[1] The anisotropic force field that binds such complexes aligns the two molecules regioselectively, thus offering a novel means of studying entrance channel specificity. For instance, there is a qualitative structural change in CO_2–HX complexes in going from quasilinear CO_2–HCl to inertially T-shaped CO_2–HBr, and this difference provides an opportunity to study regiospecific effects in photoinitiated H atom reactions with CO_2.[2] In addition to regional selection for the reaction, photoinitiation in complexes is compatible with control of the reaction energy by varying the photolysis wavelength, as well as "setting the clock" for the reaction when using ultrashort laser pulses.[3]

In this approach to studying photoinitiated chemical reaction dynamics, having information about the structure of the complex is prerequisite to understanding the effects of entrance channel parameters on reaction probabilities, branching ratios, product state distributions, and reaction times. To obtain structural information for CO_2–HX complexes (X=F, Cl, and Br), we have used infrared spectroscopic techniques to record rovibrational spectra of complexes by exciting a single quantum of the CO_2 ν_3 asymmetric stretch mode, i.e., the (001) level in isolated CO_2.[4] CO_2–H(D)F and CO_2–H(D)Cl were found to be quasilinear (i.e., hingelike bending with large zero-point amplitudes) for both the ground and vibrationally excited states. Ground-state rotational constants were in excellent agreement with microwave spectroscopic studies of CO_2–H(D)F[5] and CO_2–H(D)Cl,[6] as well as other infrared spectroscopic results for CO_2–HF, in which the HF chromophore was excited.[7] With the latter, HF($v=1$) excitation results in a nonlinear equilibrium geometry for the intermolecular potential surface, while the potential for HF($v=0$) is very flat (i.e., dominated by quartic and sextic angular terms) and the classical turning points were shown to be at $\pm 38°$ for the zero-point energy level.[7]

On the other hand, the CO_2–HBr rovibrational absorption spectrum displayed a typical *b*-type spectrum of an asymmetric rotor, a pattern that differs dramatically from those obtained with complexes such as CO_2–HF and CO_2–HCl. Analyses indicated that the structure of CO_2–HBr is inertially T-shaped with the C–Br interatomic distance almost perpendicular to the CO_2 molecular axis. This is similar to CO_2–Ar[8] if we ignore the hydrogen atom. The structural variation in going from CO_2–HF(HCl) to CO_2–HBr was ascribed to competition between hydrogen bonding (favoring the hingelike geometry) and dispersive forces (favoring the T-shape).[4] In addition, the shift in frequency (relative to uncomplexed CO_2) of the CO_2 asymmetric stretch band origin also appeared to correlate with the

[a]Present address: Battelle Pacific Northwest Lab., Battelle Blvd., P.O. Box 999, Richland, Washington 99352.
[b]Present address: Department of Chemistry, University of California, Santa Barbara, California 93106.

 0021-9606/92/205392-11$006.00

structural change, i.e., a blue shift for hingelike CO_2–H(D)F(Cl) and a small red shift for T-shaped CO_2–HBr. However, the position of the H atom in the CO_2–HBr complex was not determined. Subsequently, by comparing the nuclear quadrupole coupling constants of the bromine atom in the complex and free HBr. Rice *et al.* determined that on average the HBr axis is at an angle of $\sim 66°$ (or 114°) from the *a* axis of the complex.[9]

To further determine structural features of the CO_2–HBr complex, we have now obtained the CO_2–DBr infrared rovibrational spectrum which complements our previous studies on CO_2–HBr.[4] The position of the H(D) atom is determined from differences between the CO_2–DBr and CO_2–HBr moments-of-inertia. From this, we conclude that on average the H atom lies in the Br–CO_2 plane, with the HBr axis almost parallel to the CO_2 axis. The average structure is best described as inertially T shaped and planar with roughly parallel CO_2 and HBr axes.[10] This differs, though not dramatically, from the result of Rice *et al.*, who inferred an angle of about 24° between the directions of the HBr and CO_2 axes.[9]

The Kraitchman method[11] used for locating atoms in rigid molecules may not be appropriate if the intermolecular vibration is too anharmonic or asymmetric upon displacement from the equilibrium position, or if the intermolecular vibration has too large an amplitude. Thus, it is important to examine directly the intermolecular interaction potential of the complex. This potential holds the key to understanding the behavior of the complex; without it there is too much latitude in reconciling data. To gain insight into the anisotropic force field binding the CO_2–HBr complex, to determine the equilibrium geometry of the ground state complex, and to provide the intermolecular potential surface, we have carried out *ab initio* computations by using Møller–Plesset second-order perturbation (MP2) methods[12] with double zeta plus double polarization basis sets. The results of the calculations, corrected for basis set superposition errors, are in accord with the experimental results derived from the isotopic substitution. They are consistent with an equilibrium geometry with the Br–H bond essentially parallel to the O–C–O axis. Though these computations are lengthy, we have determined portions of the potential energy surface about the equilibrium point with respect to rotation of the HBr both in and out of the plane of the complex, as well as R_{cm} stretching.

The potential appears to be nearly symmetric with respect to the in- and out-of-plane hydrogen rotations, with a propensity for large-amplitude H-atom zero-point excursions, which accommodate significant reactivity when the HX moiety is photoexcited with a uv photon. The barrier height for out-of-plane rotation of the HBr is fortuitously close to the experimentally determined value, and supports the hypothesis that the difference between our observed *A* constant and that obtained using microwave methods is due to the tunneling splitting caused by this rotational barrier. We then estimated the energy levels, eigenfunctions, expectation values and dispersions of the angles for the hydrogen rotations. These calculations indicate little or no in-plane tunneling and only small differences between the H and D zero-point effects on the expectation values of the angles. The small amount of in-plane tunneling for the light hydrogen atom can be ascribed to strong coupling of the HBr in-plane bend with R_{cm} stretching motion. It appears that the isotopic substitution approach should be valid for this floppy molecule in which the interaction potential is nearly symmetric with respect to the displacement from its equilibrium position. However, the angular dispersion is about eight times larger than that of a rigid molecule, so we expect the uncertainty in the structural parameters to be an order of magnitude larger than in a typical rigid molecule.

II. EXPERIMENT

The experimental arrangements have been described previously in detail.[4,13] In brief, CO_2–DBr complexes were prepared by expanding gas mixtures of CO_2/DBr/Ar (1:3:300) through a slotted pulsed nozzle (0.15×38 mm^2). The pulsed valve was operated at a rate of about 3 Hz with a pulse duration of about 1–2 ms. Rotational temperatures were typically 7–10 K.

The diode laser was operated in the temperature range 30–70 K by using a closed-cycle refrigerator. Various laser modes could be accessed by varying the temperature and by adjusting the current applied to the diode. To select a single mode, the laser output was passed through a monochromator with a bandpass of approximately 1 cm^{-1}. Small portions of the single-mode power were passed through a room-temperature reference cell containing CO_2 monomer for absolute calibration and a temperature stabilized germanium etalon, which provided fringes for relative frequency measurements. Most of the laser power (90%) was passed through the vacuum chamber for the absorption measurements. Absorption signals from the reference cell, etalon, and molecular beam were recorded simultaneously by three LN_2-cooled InSb detectors connected to three transient digitizers. The fast tunability of diode lasers enabled us to scan a region of ~ 0.3 cm^{-1} (4000 points) during a single opening of the nozzle. Each spectrum was averaged over 50–200 scans by an IBM/AT. The frequency was calibrated using CO_2 transition frequencies and the etalon fringes (free spectral range $= 0.016$ cm^{-1}). All relevant volumes and light paths were purged with nitrogen to reduce absorption of the laser radiation by CO_2 in the atmosphere.

The infrared absorption features of CO_2–DBr were recorded between 2347.0 and 2349.5 cm^{-1}, which corresponds to the asymmetric stretching mode of CO_2. Under current experimental conditions, spectral features due to clusters of CO_2 with rare gases (e.g., Ne, Ar, etc.) were prominent and often interfered with transition lines of CO_2–DBr. Hence, to obtain maximum spectral information, ultra-high purity Ar and first-run Ne gases were used alternatively as carrier gases for the supersonic expansion. All gases were obtained commercially and used without further purification.

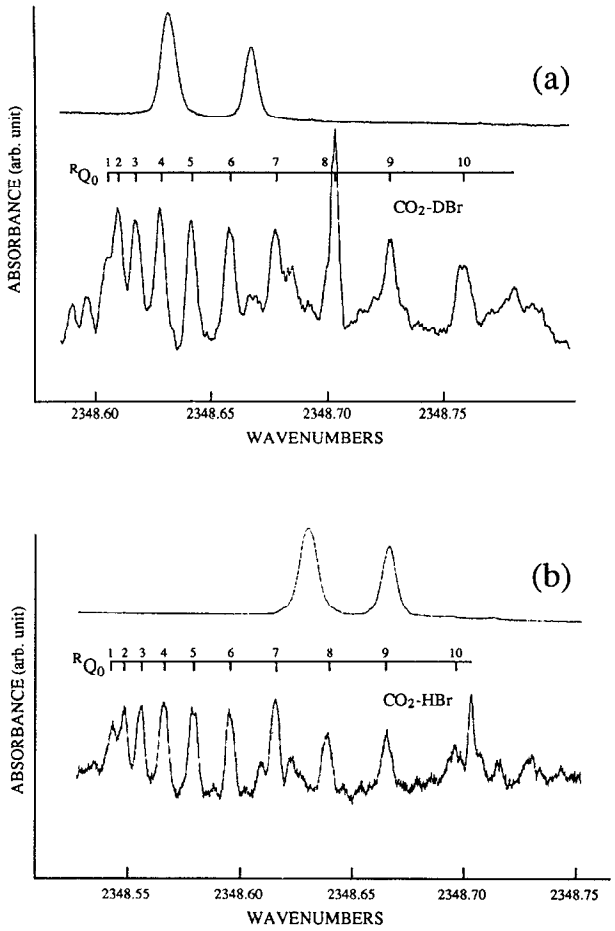

FIG. 1. Portions of (a) CO_2–DBr and (b) CO_2–HBr spectra showing prominent $^RQ_0$ branches, along with absorption features of room-temperature CO_2 monomers.

III. RESULTS AND DISCUSSION

The CO_2–DBr absorption spectrum was very similar to that of CO_2–HBr,[4] with the band origins separated by only 0.07 cm^{-1}, as shown in Fig. 1. A total of 68 transitions corresponding to $^PQ_2$, $^PP_1$, $^PQ_1$, $^RP_0$, $^PR_1$, $^RQ_0$, $^RR_0$, $^RQ_1$, and $^RR_1$ sub-bands were recorded and fit to the Watson Hamiltonian given below (the results are listed in Table I):[14]

$$H=\tfrac{1}{2}(B+C)J^2+[A-\tfrac{1}{2}(B+C)]J_a^2+\tfrac{1}{2}(B-C)(J_b^2-J_c^2) -D_J J^4-D_{JK}J^2J_a^2-D_K J_a^4. \quad (1)$$

Of the various parameters, only A, B, C, and D_{JK}, along with the fundamental band center frequency, ν_0, were included in the fit. Ground-state rotational constants were first determined by finding the combination differences for the ground-state transitions. Rotational constants for the vibrationally excited state and ν_0 were then fit to the overall transitions with the predetermined rotational constants for the ground state. D_K could not be determined with the current data because only transitions involving $K_a \leqslant 2$ have been assigned. Also, D_J was found to be zero within error limits. It should be noted that D_{JK} is larger in the ground state than in the upper state. We attempted a fit with the upper-state D_{JK} fixed at the lower-state value; however, the overall deviation from this fit was about 50% greater than with different D_{JK} in the two vibrational states. One should not attribute undue physical significance to the fitting parameters D_J, D_{JK}, and D_K. In addition, seven new transitions for CO_2–HBr complexes were found, and these lines, combined with our previous data,[4] were fit using Eq. (1). To compare the results of CO_2–HBr and CO_2–DBr consistently, the same type of parameters were included in the fits for both isotopic species. Table II summarizes the results for the moments-of-inertia, rotational constants and band origins for CO_2–DBr and CO_2–HBr.

In the rovibrational spectrum of an asymmetric rotor with b-type transitions, the A constant is directly related to the band gap between Q branches, which are the most intense absorption features in the spectrum,[15] and it can be measured quite accurately. The CO_2–DBr A constant is smaller than that of CO_2–HBr, implying that the H(D) atom is not on the a axis. If the Br positions in both complexes do not differ significantly, then the different A constants must be accounted for by the H atom being away from the a axis. The B and C rotational constants for CO_2–DBr are smaller than those for CO_2–HBr, indicating that the hydrogen is displaced from the b and c axes as well. The small inertial defects in CO_2–HBr and CO_2–DBr suggest that the complexes are planar.

In interpreting the rovibrational transitions observed in CO_2–H(D)Br complexes, nuclear spin statistics for the zero-spin oxygen atoms must be considered.[15] In CO_2–Ar, which is T-shaped with C_{2v} symmetry,[8] only half of the transitions are present, since the nuclear spin wave function can only have even symmetry, i.e., the antisymmetric states have zero statistical weight. Thus, only even K_a states are allowed in the totally symmetric ground vibrational state, while only odd K_a states are found in the excited vibrational state, which has odd symmetry, with respect to the C_2 axis. However, in the rovibrational spectrum of CO_2–D(H)Br,[4] all transitions involving both even and odd K_a are observed for the ground and the excited vibrational states. This can be explained two ways. First, the molecule has no C_2 axis of symmetry: The two oxygens are distinguishable because one is closer to the hydrogen atom than the other. The second, nearly equivalent, interpretation is that there is a possible inversion of the hydrogen atom with a substantial barrier from one form to another in the twofold structural degeneracy. In the second case, there will be nearly degenerate even and odd vibrational levels, with respect to the inversion. For the ground vibrational state, the even K_a states belong to the even inversion state, while the odd K_a levels belong to the odd inversion state. When the asymmetric stretching mode of the CO_2 group is given one quantum of energy, the rotational state symmetries switch and the converse is true for the allowed even and odd K_a values. Thus, the transitions that have been observed actually belong to two different inversion states whose energy difference vanishes as the barrier height approaches infinity. If the two states were not nearly degenerate, then the odd and even K_a states

TABLE I. Rovibrational transitions of CO_2–DBr. $\sigma_{rms}=0.0008$ cm^{-1}.

Transition							Observed	Residues	Transition							Observed	
J'	K_a'	K_c'	←	J''	K_a''	K_c''	(cm^{-1})	(cm^{-1})	J'	K_a'	K_c'	←	J''	K_a''	K_c''	(cm^{-1})	Observed–Calculated
3	1	3		3	2	2	2347.2654	−0.0002	8	0	8		7	1	7	2348.6945	−0.0009
4	1	4		4	2	3	2347.2569	0.0010	1	1	0		1	0	1	2348.6037	0.0009
5	1	5		5	2	4	2347.2435	−0.0001	2	1	1		2	0	2	2348.6083	0.0003
9	1	9		9	2	8	2347.1689	−0.0006	3	1	2		3	0	3	2348.6165	0.0006
10	1	10		10	2	9	2347.1452	0.0007	4	1	3		4	0	4	2348.6276	0.0010
11	1	11		11	2	10	2347.1172	0.0003	5	1	4		5	0	5	2348.6412	0.0008
3	1	2		3	2	1	2347.2975	0.0008	6	1	5		6	0	6	2348.6578	0.0005
4	1	3		4	2	2	2347.3079	0.0007	7	1	6		7	0	7	2348.6779	0.0000
6	1	5		6	2	4	2347.3216	0.0018	8	1	7		8	0	8	2348.7024	0.0002
6	1	6		6	2	5	2347.3358	0.0015	9	1	8		9	0	9	2348.7311	0.0004
7	1	7		7	2	6	2347.3515	0.0014	10	1	9		10	0	10	2348.7637	0.0001
9	1	8		9	2	7	2347.3833	−0.0008	11	1	10		11	0	11	2348.8004	−0.0008
0	0	0		1	1	1	2347.8564	−0.0007	12	1	11		12	0	12	2348.8439	−0.0001
1	0	1		2	1	2	2347.7755	−0.0003	2	1	2		1	0	1	2348.7649	−0.0005
2	0	2		3	1	3	2347.6965	−0.0006	3	1	3		2	0	2	2348.8439	−0.0001
3	0	3		4	1	4	2347.6215	0.0006	4	1	4		3	0	3	2348.9209	0.0009
1	0	1		1	1	0	2347.9380	−0.0004	5	1	5		4	0	4	2348.9949	0.0012
2	0	2		2	1	1	2347.9329	−0.0003	6	1	6		5	0	5	2349.0662	0.0013
3	0	3		3	1	2	2347.9240	−0.0012	7	1	7		6	0	6	2349.1347	0.0005
4	0	4		4	1	3	2347.9137	−0.0006	8	1	8		7	0	7	2349.2017	0.0000
5	0	5		5	1	4	2347.8993	−0.0011	9	1	9		8	0	8	2349.2669	−0.0008
6	0	6		6	1	5	2347.8821	−0.0012	3	2	1		3	1	2	2349.2423	−0.0004
7	0	7		7	1	6	2347.8615	−0.0011	4	2	2		4	1	3	2349.2325	−0.0004
8	0	8		8	1	7	2347.8377	−0.0002	5	2	3		5	1	4	2349.2214	0.0003
9	0	9		9	1	8	2347.8078	−0.0015	7	2	5		7	1	6	2349.1928	−0.0003
10	0	10		10	1	9	2347.7764	0.0002	8	2	6		8	1	7	2349.1780	0.0002
11	0	11		11	1	10	2347.7395	0.0012	9	2	7		9	1	8	2349.1620	−0.0003
12	0	12		12	1	11	2347.6957	0.0003	10	2	8		10	1	9	2349.1476	0.0005
5	1	5		6	0	6	2348.0457	0.0010	4	2	3		4	1	4	2349.2829	−0.0011
6	1	6		7	0	7	2347.9454	0.0004	5	2	4		5	1	5	2349.2963	−0.0008
8	1	8		9	0	9	2347.7423	0.0000	6	2	5		6	1	6	2349.3124	−0.0004
4	0	4		3	1	3	2348.3016	−0.0003	7	2	6		7	1	7	2349.3310	−0.0001
5	0	5		4	1	4	2348.3958	−0.0021	8	2	7		8	1	8	2349.3516	−0.0006
7	0	7		6	1	6	2348.5943	−0.0006	2	2	1		1	1	0	2349.4284	−0.0001

could not be fit simultaneously with a single set of parameters. Rather, two slightly different sets of parameters would be required. According to the selection rules in the rovibronic spectrum, a *b*-type spectrum is expected with $\Delta K_a=\pm 1$ transitions because the asymmetric CO_2 stretch is excited and the axis of the CO_2 moiety is parallel to the *b* axis. Based on the symmetry arguments given above, the rovibronic transitions will be between inversion levels of the same symmetry, i.e., the observed transitions are within the same manifold of the inversion states shown in Fig. 2.

Recent Fourier transform microwave spectroscopic studies of CO_2–HBr by Rice *et al.*, in which they report a *b*-type microwave spectrum, provide further evidence for a barrier to H-atom tunneling.[9] Their *B* and *C* rotational constants are the same as ours to within our experimental error, but their *A* moment is 1186 MHz larger than our value. Since the selection rules for the *pure* rotational transitions are $\Delta K_a=\pm 1$, they observe only transitions between symmetric and antisymmetric inversion levels, i.e., between the two manifolds depicted in Fig. 2. They interpret the 1186 MHz deviation in the *A* moment as the separation between the two inversion states. However, they have not yet observed the microwave spectrum of the deuterated species. Since only the *A* moment is affected by the inversion, the tunneling motion must involve the hydrogen rotating out of the plane of the molecule. The *ab initio* calculations described below substantiate this conclusion.

TABLE II. CO_2–D(H)Br constants for the ground and excited vibrational states.

	CO_2–DBr	CO_2–HBr[a]
Ground state		
A'' (MHz)	11190.9(40)	11594.3(35)
B'' (MHz)	1375.55(52)	1384.58(35)
C'' (MHz)	1219.78(65)	1230.87(39)
D_{JK}'' (MHz)	0.91(9)	0.27(10)
Δ'' (amu Å^{-2})	1.76	1.99
Excited state		
A' (MHz)	11168.9(37)	11503.5(44)
B' (MHz)	1375.47(17)	1383.47(21)
C' (MHz)	1218.74(14)	1230.47(18)
D_{JK}' (MHz)	0.16(7)	0.24(10)
Δ' (amu Å^2)	2.00	1.49
ν_0 (cm^{-1})	2348.2710(2)	2348.2016(2)
$\Delta\nu$ (cm^{-1})[b]	−0.8723	−0.9417

[a]The values presented here are slightly different from those reported previously,[4] due to the inclusion of seven new transition lines and D_{JK} in the present fit.

[b]$\Delta\nu$ is defined as ν_0(complex)−ν_0(monomer).

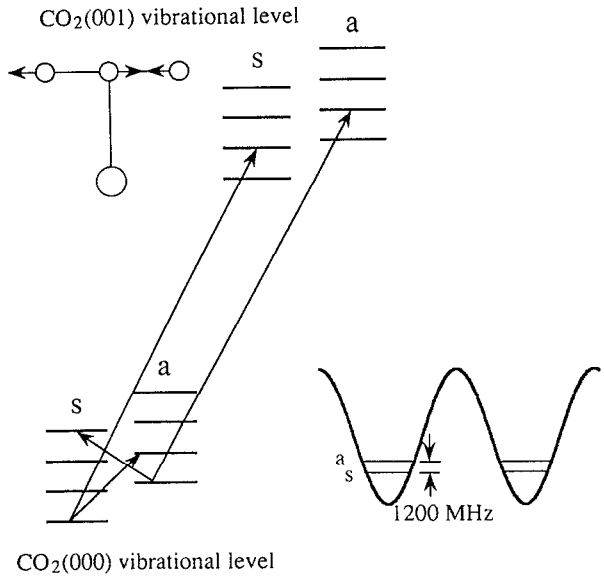

FIG. 2. Schematic of energy levels involved in the observed transitions in CO_2–HBr. Long lines indicate rovibrational transitions observed in infrared absorption spectra; short lines represent pure rotational transitions observed in microwave spectra. Labels *s* and *a* refer to symmetric and antisymmetric inversion levels, respectively.

In the structural determination from the rotational constants, it is assumed that the monomers are rigid and the complex is planar. Figure 3 depicts the geometrical parameters, $R_{c.m.}$, R_{CBr}, r, θ_1, θ_2, θ_{BrCO}, and θ_{HBrC}. The distance $R_{c.m.}$ between the center-of-masses of the two constituents depends only on the moment-of-inertia about the c axis, and can be calculated from[16]

$$\mu R_{c.m.}^2 = I_c - I_1 - I_2 , \tag{2}$$

where $\mu = M_1 M_2/(M_1+M_2)$ is the reduced mass of the complex, and I_1 and I_2 are the moments-of-inertia for monomers 1 and 2, respectively. To locate the H atom, we used the difference between the CO_2–HBr and CO_2–DBr moments-of-inertia assuming (i) no structural changes

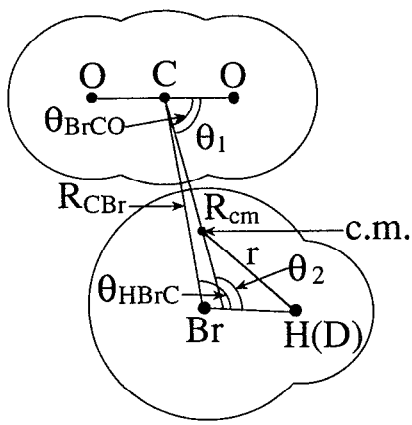

FIG. 3. Schematic drawing showing the parameters, $R_{c.m.}$, R_{CBr}, r, θ_1, θ_2, θ_{BrCO}, and θ_{HBrC} of the planar CO_2–H(D)Br complex.

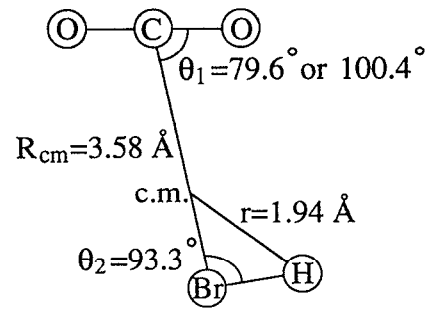

FIG. 4. Experimental geometry for ground state CO_2–HBr.

upon deuteration, and (ii) planarity. An average distance, r, from the H atom to the center-of-mass of the complex can be calculated from the Kraitchman equation[11]

$$r^2 = \frac{(M+\Delta m)}{M\Delta m}(I_c' - I_c), \tag{3}$$

where M is the mass of the complex before isotopic substitution and Δm is the mass change upon isotopic substitution; I_c' and I_c are moments-of-inertia of the isotopically substituted and original species, respectively, about the c principal axis. In principle, r can be calculated by using either I_c or the sum of I_a and I_b, but we prefer using I_c because I_a may have a small tunneling contribution. Also, we have calculated the a and b center-of-mass coordinates of the hydrogen atom independently of each other by using other Kraitchman equations.[16] These results were in close agreement with the values obtained from Eq. (3). Then θ_2 is obtained from simple geometrical considerations as shown in Fig. 4. Finally, θ_1 is obtained from[4,17]

$$\sin^2\theta_1 = \frac{I_a(I_c-I_a)}{I_1(I_c-I_1-I_2)} - \frac{I_2}{I_1}\sin^2\theta_2 - \frac{I_2}{(I_c-I_1-I_2)}\sin^2(\theta_1+\theta_2). \tag{4}$$

Equation (4) yields two θ_1 values, and whether OCO is tilted towards or away from the hydrogen atom is unknown. The final structural parameters, R_{CBr}, θ_{BrCO}, and θ_{HBrC} for both the ground and excited vibrational states, are given in Table III along with the theoretical ground state geometry.

TABLE III. Structural parameters of CO_2–HBr and CO_2–DBr (parentheses).

	Experimental		Theoretical
	Ground state	Excited state	Ground state[a]
R_{CBr} (Å)	3.579(3.581)	3.580(3.580)	3.62
θ_{BrCO} (deg)	79.8	79.7	88.8
θ_{HBrC} (deg)	93.1	96.3	85.9

[a]The T-shaped geometry was optimized at the MP2 level (double-zeta plus double polarization basis sets) and corrected for basis set superposition errors.

The CO_2–H(D)Br complex has an average structure in which the H(D)–Br bond is roughly parallel to the CO_2 molecular axis. A similar structure has also been observed for the CO_2 dimer.[10] However, other CO_2-containing complexes such as CO_2–N_2,[18] CO_2–HCN,[16] and CO_2–CO[19] have T-shaped structures, with the molecular axis of the other moiety perpendicular to the CO_2 molecular axis. Such arrangements preserve C_{2v} symmetry, thereby disallowing odd K_a states in the ground vibrational state and even K_a states in the excited state (CO_2 asymmetric stretch). In fact, CO_2–H(D)Br is the first inertially T-shaped CO_2-containing complex in which all K_a states are present in rovibrational spectra.

It is interesting to compare frequency shifts for the different CO_2–HX band origins relative to CO_2 monomer (2349.143 26 cm^{-1}). The band origin of CO_2–D(H)Br is red shifted by 0.872 cm^{-1}, while for CO_2–HF and CO_2–HCl hingelike complexes, the inequivalency in the two CO bonds results in blue shifts of 9.98 and 3.87 cm^{-1}, respectively.[4] On the other hand, in T-shaped complexes such as CO_2–Ar[8] and CO_2–HBr,[4] there is relatively little effect on the CO_2 asymmetric stretching frequency. In the homologous series of CO_2–Rg complexes (Rg=Ne, Ar, Kr, and Xe),[8] where dispersive forces dictate the structures, the band origin associated with the CO_2 asymmetric stretch mode shifts toward lower frequencies in going from Ne to Xe, a trend that correlates with the increasing polarizabilities.[8] Hence, it is reasonable to attribute the red shift of the CO_2 asymmetric stretch in CO_2–H(D)Br to the large polarizability of Br. A rather small separation between CO_2–HBr and CO_2–DBr band origins (0.07 cm^{-1}), compared with CO_2–H(D)F (0.52 cm^{-1}) and CO_2–H(D)Cl (0.83 cm^{-1}),[4] suggests that the Br–CO_2 interaction is more important than the H–CO_2 interaction.

IV. *AB INITIO* CALCULATIONS

Valence double-zeta basis sets were used for carbon (9*s*5*p*/3*s*2*p*) and oxygen (9*s*5*p*/3*s*2*p*),[20] with one set of d-polarization functions for carbon and oxygen [ζ^d(C) $=0.73$ and ζ^d(O)$=1.07$] optimized for CO_2 at the HF level and augmented with one set of diffuse *d* functions [ζ^d(C)$=0.17$ and ζ^d(O)$=0.287$]. Unscaled valence double-zeta basis sets were used for hydrogen (4*s*/2*s*),[20] augmented with one set of p-polarization functions (ζ^p $=0.6$) and one set of diffuse p functions ($\zeta^p=0.2$). Double-zeta basis sets for bromine (3*s*3*p*/2*s*2*p*) with effective core potentials[21] were used with one set of *d*-polarization functions ($\zeta^d=0.45$) optimized for HBr at the GVB(1/2) level and augmented with one set of diffuse d functions ($\zeta^d=0.15$).

Experimental equilibrium geometries of CO_2 (R_{CO} $=1.1621$ Å)[22] and HBr ($R_{HBr}=1.413$ Å)[23] were used, and the CO_2–HBr equilibrium geometry was determined at the MP2 level. Basis set superposition error (BSSE) was accounted for by using the counterpoise method.[24] The calculated ground state equilibrium geometry is shown in Fig. 5 and listed in Table III. Table IV summarizes total energies.

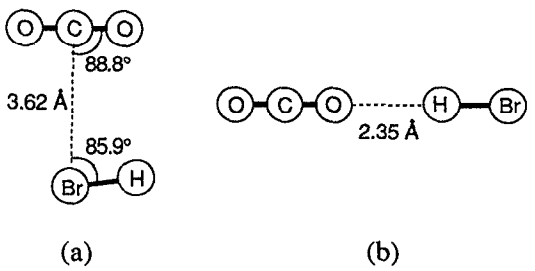

FIG. 5. Theoretical geometries for (a) T-shaped and (b) linear CO_2–HBr. Calculations were at the MP2 level (double-zeta plus double polarization basis sets); basis set superposition errors were corrected by using the counterpoise method.

Figure 6 shows potential energy contours for planar, inertially T-shaped complexes as a function of C–Br distance, R_{CBr}, and Br–C–O angle, θ_{BrCO}, with the HBr and CO_2 axes parallel (i.e., $\theta_{HBrC}=\pi-\theta_{BrCO}$). A minimum energy of -392 cm^{-1} is found at $R_{CBr}=3.62$ Å and θ_{BrCO} $=88.8°$.

For planar structures, the dependence of the potential on θ_{HBrC} is shown in Fig. 7 for two slices in the potential energy surface: (1) with R_{CBr} fixed at 3.62 Å (dashed curve), and (2) with R_{CBr} allowed to change to minimize the energy (solid curve). For planar complexes with θ_{BrCO} fixed at 88.8°, $\theta_{HBrC}=83.7°$ is the minimum energy value with $R_{CBr}=3.62$ Å, while $\theta_{HBrC}=85.9°$ is the optimized value when the R_{CBr} distance is relaxed to give a minimum potential. Note that the potential is quite flat with respect to θ_{HBrC} near these minima (see Fig. 7). When R_{CBr} was relaxed to give a minimum potential for the in-plane H bend, a rotational barrier of 312 cm^{-1} was obtained at $\theta_{HBrC}=180°$ and $R_{CBr}=3.87$ Å. On the other hand, the intermolecular potential at $\theta_{HBrC}=0°$ was repulsive and unbound in the R_{CBr} coordinate. Figure 8 displays the value of R_{CBr} at the minimum energy as θ_{HBrC} varies from 0° to 180° in the molecular plane. R_{CBr} remains almost unchanged from the equilibrium distance of 3.62 Å over a wide range of angular variation near the equilibrium angle of $\theta_{HBrC}=85.9°$. The calculated equilibrium distance of $R_{CBr}=3.62$ Å is in good agreement with the experimental value of $\langle R_{CBr}\rangle=3.58$ Å, and the bond angles of θ_{BrCO} $=88.8°$ and $\theta_{HBrC}=85.9°$ are also in reasonable agreement with the experimental results depicted in Fig. 4.

Figure 9 shows the variation of the potential energy while varying the out-of-plane angle (φ) for fixed values of $R_{CBr}=3.62$ Å and $\theta_{BrCO}=88.8°$. Thus, at equilibrium, the H atom clearly lies in the Br–CO_2 plane. The twofold rotational barrier for out-of-plane H bend (184 cm^{-1}) is significantly lower than the barrier for the in-plane H bend (312 cm^{-1}).

The planar equilibrium geometry obtained from *ab initio* calculations substantiates the planarity assumption used in the structural determination from the experimental rotational constants. Calculated rotational constants (equilibrium values) are $A=0.373\,14$, $B=0.045\,31$, and C $=0.040\,40$ cm^{-1}, while the experimental values (i.e., averaged over the ground vibrational state) are 0.386 74,

TABLE IV. Total energies (hartrees) and binding energies (cm^{-1}) for linear and T-shaped CO_2–HBr complexes and their subsystems. All geometries are given in Fig. 5 and Sec. IV. Here, CO_2(HBr) represents the CO_2 molecule with basis sets for HBr but without any potentials for HBr. In both cases, geometries were optimized at the MP2 level (double-zeta plus double polarization basis set).

Molecules	Level			
	HF (h)	ΔE (cm^{-1})[b]	MP2 (h)	ΔE (cm^{-1})[a]
		Linear		
CO_2–HBr	−201.208 684	−223(−321)	−201.839 283	−517(−860)
CO_2(HBr)	−187.683 412		−188.172 874	
HBr(CO_2)	−13.524 257		−13.664 055	
		T-shaped		
CO_2–HBr	−201.208 094	−60(−186)	−201.838 466	−392(−680)
CO_2(HBr)	−187.683 271		−188.172 388	
HBr(CO_2)	−13.524 551		−13.664 292	
		Free		
CO_2	−187.683 021		−188.171 811	
HBr	−13.524 201		−13.663 554	

[a]$\Delta E = E(CO_2\text{–HBr}) - E[CO_2(HBr)] - E[CO_2(HBr)]$ is in unit of cm^{-1} and binding energies in parentheses are with basis set superposition errors.

0.046 18, and 0.041 06 cm^{-1}, respectively. Force constants obtained from simple one-dimensional fits to the curves shown in Figs. 6, 7, and 8 yield vibrational frequencies of 42 cm^{-1} for the R_{CBr} stretch, 50 cm^{-1} for the θ_{BrCO} bend (also seen as lateral slipping), 65 cm^{-1} for the θ_{HBrC} bend, and 75 cm^{-1} for the φ bend. This corresponds to approximate values of 0.2 Å, 7°, 25°, and 27°, respectively, for the magnitudes of the corresponding zero-point displacements (i.e., half-width, half-maximum values). The optimum linear structure is strictly linear, with a hydrogen–oxygen distance of 2.35 Å. The binding energy (D_e) of the T-shaped complex is 392 cm^{-1} at the MP2 level, while that of the linear structure is 517 cm^{-1}. We expect a significant barrier between these isomers. Only the inertially T-shaped isomer has been observed so far.

V. EVALUATION OF THE ACCURACY OF THE STRUCTURE DETERMINATION

From the orientation of the nuclear quadrupole moment relative to the principal axes, Rice *et al.* determined that the H–Br bond forms an angle of ~66° with respect to the *a* axis of the complex.[9] An angle of ~114° is also allowed from their data, but is considered unlikely. On the other hand, the isotopic substitution method yields a value of about 90° for this angle. Thus, there is concern over which value is most representative of the hydrogen location. It was partially this concern which encouraged us to carry out the *ab initio* calculations described in the last

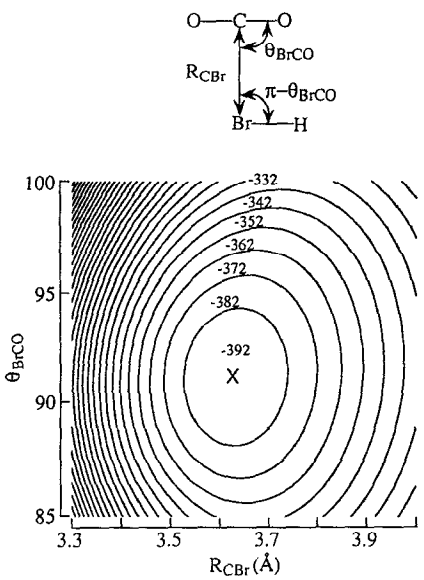

FIG. 6. Potential contours for T-shaped CO_2–HBr as a function of R_{CBr} and θ_{BrCO} with HBr and OCO kept parallel (i.e., $\theta_{HBrC} = \pi - \theta_{BrCO}$). Calculations were at the MP2 level and were corrected for BSSE. The minimum of −392 cm^{-1} is at $R_{CBr} = 3.62$ Å and $\theta_{BrCO} = 88.8°$. Contour spacing is 10 cm^{-1}.

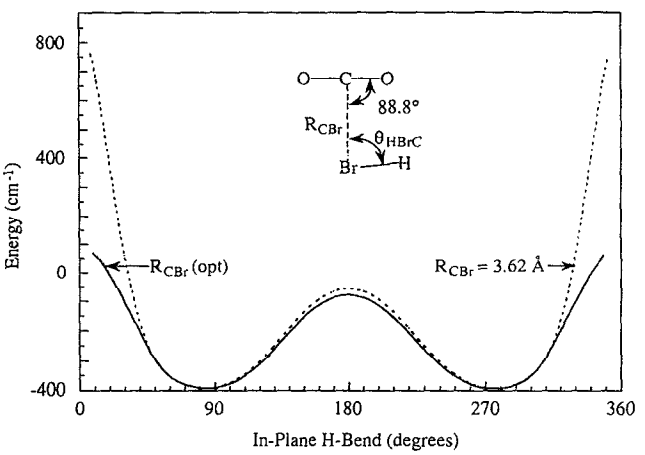

FIG. 7. Potential curves as a function of θ_{HBrC} (in-plane H bend) for T-shaped CO_2–HBr (MP2 level with BSSE corrections). The dashed curve is a best fit to the calculated potentials with Br and CO_2 held at their equilibrium values; the solid curve represents a best fit to the minimum potential with the carbon–bromine distance relaxed to minimize the energy.

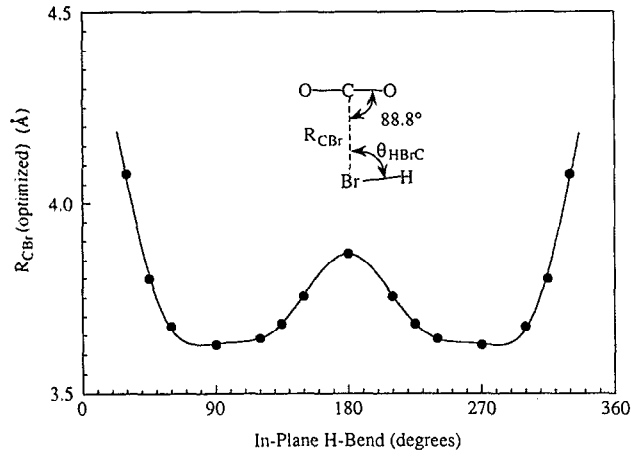

FIG. 8. Optimized R_{CBr} distance vs θ_{HBrC} for T-shaped CO_2–HBr (MP2 level with BSSE corrections). R_{CBr} was energy optimized at each θ_{HBrC}.

section. We have now used slices of the *ab initio* potential surface to check the validity of the isotopic substitution method.

Structural determination methods were originally developed for well-behaved rigid molecules. Depending on the amount of data available, various methods are applicable. With minimal data, one of the most reliable methods is using differences in moments-of-inertia upon isotopic substitution.[11] Qualitatively, the rationalization for the reliability of this method is based on a Taylor series expansion of the effective moments-of-inertia about the equilibrium value, and the argument that upon isotopic substitution, the higher order terms do not change appreciably.[25] Thus, when differences in the moments-of-inertia are computed, the correction terms tend to cancel and coordinates closer in magnitude to r_e are obtained. This approximation works

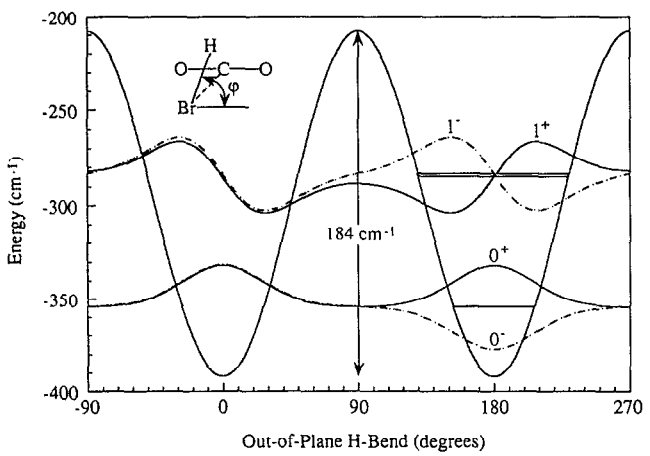

FIG. 9. Potential as a function of φ (out-of-plane H bend) for T-shaped CO_2–HBr (MP2 level with BSSE corrections). Br and CO_2 were kept at the equilibrium geometry. Vibrational wave functions are also included. Solid curves represent symmetric wave functions and dashed curves represent antisymmetric wave functions. The splitting between the 0^+ and 0^- states is about 0.072 cm^{-1} (2160 MHz).

best when isotopic substitution occurs on heavy atoms. It is least valid for hydrogen, where differences in zero-point effects are large upon deuteration, i.e., substituting D for H shortens average bond lengths by 0.003–0.005 Å.[26]

For floppy van der Waals complexes, the meaning of structure becomes more diffuse and structure determinations are less meaningful. Essentially, the equilibrium structural parameters represent one or more minima on the molecule's potential energy surface, but the molecule may spend little time at the equilibrium position. The validity of the structure concept depends on whether the vibrational energy levels lie well below, are comparable to, or lie well above the barriers separating the minima in the complex's potential surface. In the simplest of terms, the *effective* rotational constants obtained from fitting a spectrum are some complicated function of the structural parameters averaged over the vibrational state. Thus, an estimate of the floppiness of the complex is required to evaluate the validity of the structure determination.

The proper theoretical treatment of these cases depends on the degree of floppiness of the complex, which could vary from semirigid to free internal rotation. The less floppy cases with large amplitude (but coupled) motions have been adeptly treated by Bunker and co-workers with a series of bender Hamiltonians.[27–29] In these cases, the Hamiltonian is no longer separable into the rotational and vibrational parts. Rather, the large amplitude bending and the rotation must be treated simultaneously. These Hamiltonians, called the rigid-, semirigid-, and nonrigid-bender Hamiltonians, have increasing degrees of complexity. The nonrigid-bender Hamiltonian has been used for quasilinear symmetric triatomics and quasiplanar polyatomics, such as ammonia. In the semirigid-bender, most of the parameters are held fixed and parametrized: Thus, only variations of parameters with the bend are retained. However, in all three cases, the energies of numerous vibrational states must be available prior to calculations. When the two moieties become nearly uncoupled and freely rotating with respect to each other, other approaches, such as those pioneered by Bratoz and Martin[30] and by Le Roy and Carley,[31] must be employed. In these cases, again, the potential energy surface must be well characterized prior to solving the equations, or it must be obtained by iterative procedures.

More elaborate schemes have been developed to determine the actual rovibrational energy levels of floppy complexes without approximations;[32] however, the potential energy surface must be known. Thus, these techniques have been only applied to systems with few structural variables such as Rg–diatomics, Rg–triatomics, or diatomics–diatomics. For a system such as CO_2–HBr with a four dimensional intermolecular potential surface, the computational costs to obtain a full *ab initio* surface are prohibitive.

Though we have insufficient data to use confidently the semirigid-bender approach, from the theoretically calculated partial potential surface, we can get some indication of the errors involved in locating the hydrogen atom by using the Kraitchman method.[11] For this method to be

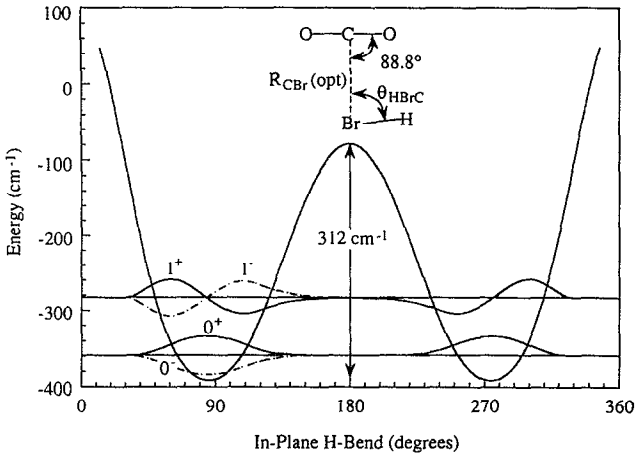

FIG. 10. Vibrational wave functions as a function of θ_{HBrC} (in-plane H bend) for T-shaped CO_2–HBr. The potential used is the solid curve in Fig. 7. Solid curves represent symmetric wave functions and dashed curves represent antisymmetric wave functions. The splitting between the 0^+ and 0^- states is about 0.0004 cm^{-1} (12 MHz).

valid, (i) there must be little or no tunneling of the hydrogen between the two equivalent positions, i.e., the wave function is zero under the potential barrier. (ii) There must be only small deviations in vibrationally averaged structural parameters between the hydrogen and deuterium isotopomers. And (iii) the quantum mechanical dispersion in the angle θ, $\Delta = |\langle v|\theta^2|v\rangle - \langle v|\theta|v\rangle^2|^{1/2}$, must be about the same for the hydrogen and deuterium species. The latter is an estimate of the amplitude of motion in the potential well. In order to estimate the errors incurred by using the Kraitchman method to locate the hydrogen atom, we have used a computer program, ASTORT, developed by Groner and Durig,[33] which solves the one dimensional Hamiltonian for a cyclic potential,

$$[F(\theta)p_\theta^2 + V(\theta)]\psi(\theta) = E_v\psi(\theta), \tag{5}$$

where θ is the internal rotation variable, $F(\theta)$ represents the angle dependent reduced moment-of-inertia of the complex (the G matrix element), expressed as a truncated 16-term Fourier series, and $V(\theta)$ is the potential energy expressed as a six-term Fourier series,

$$V(\theta) = \frac{1}{2}\sum_n V_n(1-\cos n\theta). \tag{6}$$

$F(\theta)$ takes into account the changes in structural parameters as an asymmetric internal rotor angle, θ, reorients itself. The Hamiltonian is diagonalized in a truncated free rotor basis where sufficient terms are retained to converge the lower energy levels. Figures 9 and 10 show the calculated vibrational energy levels and wave functions in the two internal rotation potentials. The program was modified to calculate expectation values of θ and θ^2, as well as the angular dispersion Δ. The results are summarized in Table V.

For out-of-plane rotation of the HBr about the R_{cm} axis, a $\cos 2\phi$ potential form was assumed. The intermolecular distance R_{cm} was held constant. For the calculated barrier height of 184 cm^{-1}, the splitting of the first two levels is 0.072 cm^{-1} or 2159 MHz. In fact, by fitting the height of the potential barrier to the observed value of 1186 MHz mentioned in Sec. III, a barrier height of 214 cm^{-1} is determined, fortuitously close to the theoretical value. Thus, the difference in energy between the two levels is very sensitive to the barrier height and the shape of the potential, as well as the actual structure of the complex. This agreement supports the hypothesis that the observed splitting originates from out-of-plane rotation of the HBr with respect to the CO_2. The energy levels of the deuterated species are also given in Table V.

TABLE V. Energy levels and expectation values for the potential given in Figs. 7 and 9.

	In-plane rotation							
	CO_2–HBr				CO_2–DBr			
Vibrational level	Energy (cm^{-1})	$\langle\theta\rangle$ (deg)	$\sqrt{\langle\theta^2\rangle}$ (deg)	Δ (deg)	Energy (cm^{-1})	$\langle\theta\rangle$ (deg)	$\sqrt{\langle\theta^2\rangle}$ (deg)	Δ (deg)
0 (0^+)	32.63308	85.5	86.9	15.6	25.37627	85.8	86.9	13.9
1 (0^-)	32.63350	85.5	86.9	15.6	25.37627	85.8	86.9	13.9
2 (1^+)	108.57921	84.2	88.6	27.5	83.35091	86.9	90.2	24.1
3 (1^-)	108.59579	84.2	88.6	27.5	83.35111	86.9	90.2	24.1
	Out-of-plane rotation							
	CO_2–HBr				CO_2–DBr			
Vibrational level	Energy (cm^{-1})	$\langle\theta\rangle$ (deg)	$\sqrt{\langle\theta^2\rangle}$ (deg)	Δ (deg)	Energy (cm^{-1})	$\langle\theta\rangle$ (deg)	$\sqrt{\langle\theta^2\rangle}$ (deg)	Δ (deg)
0 (0^+)	37.73785	0.0	20.2	20.2	25.44384	0.0	16.9	16.9
1 (0^-)	37.80989	0.0	20.2	20.2	25.44435	0.0	16.9	16.9
2 (1^+)	106.89970	0.0	36.5	36.5	74.17647	0.0	30.4	30.4
3 (1^-)	108.71558	0.0	36.5	36.5	74.19954	0.0	30.4	30.4

For in-plane θ_{HBrC} motion, the energy levels were calculated for the lower potential curve shown in Fig. 7. The energy levels and the wave functions for the lowest levels are shown in Fig. 10. The two lowest vibrational levels are degenerate to within 12 MHz. Since the amplitude of the vibrational wave function is almost zero under the in-plane rotational barrier, the transmission probability of the tunneling is negligible. The expectation value $\langle\theta_{HBrC}\rangle$ is 85.5° (close to the equilibrium θ_{HBrC} angle of 85.9°); $\langle\theta^2_{HBrC}\rangle^{1/2}$ =86.9°; and $\Delta=\pm15.6°$. Deuterium substitution yields $\langle\theta_{DBrC}\rangle=85.8°$; $\langle\theta^2_{DBrC}\rangle^{1/2}=86.9°$; and $\Delta=\pm13.9°$. For comparison, in a rigid molecule with a hydrogen vibrational frequency of 1000 cm^{-1}, the dispersion is computed to be about 2°. Thus, the complex is an order of magnitude floppier than a rigid molecule, so we assume that the uncertainty in the structure parameters is an order of magnitude larger than those in a rigid molecule.

The R_{CBr} stretching vibration is strongly coupled to in-plane H bending. As hydrogen rotates in-plane towards the OCO, R_{CBr} extends toward a new energy minimum. With this motion taken into account, the dissociation limit of the complex provides an absolute upper bound to the barrier at the $\theta=0°$ point (see Fig. 10). Because the reduced G matrix element for this motion is very large, tunneling effects will be very small and the zero-point energy low, even for a barrier height of 312 cm^{-1}. That is, tunneling via either $\theta=0°$ or $\theta=180°$ consists not only of hydrogen motion, but also consists of dragging the bromine atom as well.

In conclusion, (i) there is little tunneling of the hydrogen through the in-plane barrier, (ii) the observed tunneling splitting originates from out-of-plane rotation of HBr relative to CO_2, and (iii) there are only small deviations in $\langle\theta\rangle$ between the hydrogen and deuterium isotopomers. Thus, we believe that the most reliable $CO_2H(D)Br$ structure that can be determined with the available data has been obtained. A more accurate structure determination will require knowledge of the intermolecular vibrational states, i.e., the shape of the potential energy surface about the minimum. The large quantum mechanical dispersion indicates sizable errors in angles determined by the isotopic substitution method. Nevertheless, the value of 66° (or 114°) obtained by Rice *et al.* from comparison of electric quadrupole moments of the Br nuclei is outside the error bound revealed by the dispersion. Presently, we cannot account for this difference.

VI. SUMMARY

We have determined the average hydrogen position from the rotational constants for CO_2–DBr and CO_2–HBr complexes derived from their high-resolution rovibrational spectra. The experimental geometry of the ground state complex is inertially T-shaped, with the Br–C line essentially perpendicular to the CO_2 axis and the H–Br bond essentially parallel to the CO_2 molecular axis. The theoretical equilibrium geometry for the T-shaped complex obtained by using MP2 methods is in excellent agreement with experiment. The theoretical result of the planar complex structure validates the planarity assumption used in the experimental structure determination. The linear isomer, which has not been observed experimentally, is calculated to be as stable as the T-shaped isomer. From theoretical potential curves, we find that the H atom undergoes very large amplitude bending in the Br–CO_2 plane, i.e., a value of 50° FWHM for the zero-point θ_{HBrC} displacement. The θ_{HBrC} angle of H-atom approach toward oxygen plays a major role in determining reactivity following photoinitiation in such complexes, and large-amplitude θ_{HBrC} bend can accommodate a significant percentage of reactive events, as discussed below.[34]

The information obtained in the present study takes us one step further toward a quantitative understanding of photoinitiated CO_2–HX reactions, particularly those aspects associated with the entrance channel. Following $n\rightarrow\sigma^*$ excitation of the HX chromophore, linear CO_2–HCl complexes are very *unreactive*, yielding ~40 times less OH product than CO_2–HBr,[2] and this can be understood by considering the four-atom HOCO potential surface. End-on H-atom attack of CO_2 confronts a repulsive potential[34] and compresses preferentially the CO bond nearest the H atom. This CO bond compression makes it difficult to form a HOCO intermediate (at equilibrium, $R_{HO-CO}=1.339$ Å, compared to $R_{CO}=1.1621$ Å for CO_2).[35] Furthermore, end-on attack does not encourage bending, so again it is hard to form HOCO (at equilibrium, $\theta_{OCO}=127.6°$ and $\theta_{COH}=108.1°$).[35] Thus, it is easy to see why end-on attack is unreactive for the four-atom $H+CO_2$ system, and in addition the large chlorine–carbon distance does not encourage further chemical interactions, as may be the case with CO_2–HBr.

In the case of CO_2–HBr, the experimental and theoretical evidence presented above point toward a planar equilibrium structure in which the CO_2 and HBr axes are roughly parallel, with the Br atom facing the carbon. Photoexcitation results in two almost degenerate potential surfaces, of A' and A'' symmetries, corresponding to in-plane and out-of-plane orientations of the singly-occupied Br nonbonding p orbital, respectively. Because of the near-parallel equilibrium structure, in most cases the H-atom just flies out into the vacuum chamber and doesn't react with anything. However, as mentioned above, the very large H-atom zero-point displacements ensure that in some cases the H atom approaches the oxygen. Moreover, this large-amplitude hydrogen excursion toward the oxygen occurs without extending the C–Br distance, as illustrated in Fig. 8. As the BrH bond expands, the A' and A'' surfaces remain essentially degenerate until the H atom gets close enough to the CO_2 to begin forming HOCO. At this point, the bromine–carbon interaction becomes weakly attractive for the A' surface and weakly repulsive for the A'' surface. Consequently, reactions on the A'' surface are very much like their four-atom $H+CO_2$ analogs, but from a limited set of entrance channel parameters. Note that the broadside approach is favorable because it bends the CO_2 and even stretches the CO bond under attack, movements which bring the nuclei closer to the desired HOCO intermediate, thus promoting reaction. This steric or regiospe-

cific effect can rationalize the experimental findings qualitatively.

For the A' surface, there is clearly attraction between Br and HOCO, but at this time we can only speculate on how this might influence the dynamics. On the one hand, there is a tendency for Br and HOCO to recoil from one another because of the squeezed-atom effect.[36] Thus, it may be that the chemistry on the A' surface is similar to that on the A'' surface. On the other hand, if this push does not overcome the bromine–carbon attraction, a highly excited Br–C(O)–OH intermediate will be formed. However short-lived, this will influence the dynamics qualitatively, and may help account for observations such as the surprisingly long OH production times,[3] and a significant percentage of rotationally cold OH molecules.[1] Presently, this question might best be answered by dynamics calculations that concentrate on the entrance channel.

It is unfortunate that we have been unable to date to observe the linear isomer spectroscopically. This might be due to the energy of this isomer being higher than that of the T-shaped complex, or to rapid predissociation which would broaden the spectral lines thus making them hard to detect. We deem the latter unlikely because the O–H bond will be weaker in linear CO_2–HBr than in the cases of CO_2–HCl and CO_2–HF, both of which are readily detected. If it becomes possible to prepare and isolate linear CO_2–HBr, this will make possible several elegant experiments.

In closing, we point out that the clear regiospecific effect on reaction probability observed experimentally for photoinitiated CO_2–HCl and CO_2–HBr complexes can be rationalized by consideration of the four-atom and five-atom potential surfaces. There is a clear steric effect, attributable to the four-atom $H+CO_2$ system, with broadside H atom approaches favored over end-on attack. However, there is still ambiguity about the extent to which Br–C(O)–OH intermediates participate. The same general principles of regioselectivity apply to photochemistry in liquids and on surfaces, where mechanisms may also differ from their gas-phase counterparts.

ACKNOWLEDGMENTS

The authors benefited greatly from discussions with H. S. Taylor, W. A. Goddard III, R. D. Suenram, G. T. Fraser and J. K. Rice. We are indebted to P. Groner for a copy of his ASTORT program and for his assistance in getting the program working on our VAX computer. We are also grateful to the Materials and Molecular Simulation Center of the Beckman Institute, California Institute of Technology for the computer time. Research was supported by the U.S. Army Research Office under the auspices of the Center for the Study of Fast Transient Processes, the Department of Energy under Grant Nos. DE-FG03-89ER4053 (R.A.B.) and DE-FG03-85ER13363 (C.W.), and the National Science Foundation under Grant No. CHE-8822067 (C.W.).

[1] (a) C. Wittig, S. Sharpe, and R. A. Beaudet, Acc. Chem. Res. **21**, 341 (1988); (b) S. K. Shin, Y. Chen, S. Nickolaisen, S. W. Sharpe, R. A. Beaudet, and C. Wittig, *Advances in Photochemistry*, edited by D. Volman, G. Hammond, and D. Neckers (Wiley, New York, 1991), Vol. 16, pp. 249–363.

[2] S. K. Shin, Y. Chen, D. Oh, and C. Wittig, Phil. Trans. R. Soc. Lond. A **332**, 361 (1990).

[3] (a) N. F. Scherer, L. R. Khundkar, R. B. Bernstein, and A. H. Zewail, J. Chem. Phys. **87**, 1451 (1987); (b) N. F. Scherer, R. B. Sipes, R. B. Bernstein, and A. H. Zewail, J. Chem. Phys. **92**, 5239 (1990); (c) A. H. Zewail, Scientific Am. **263**, 76 (1990).

[4] S. W. Sharpe, Y. P. Zeng, C. Wittig, and R. A. Beaudet, J. Chem. Phys. **92**, 943 (1990).

[5] (a) F. A. Baiocchi, T. A. Dixon, C. H. Joyner, and W. Klemperer, J. Chem. Phys. **74**, 6544 (1981); (b) J. A. Shea, W. G. Read, and E. J. Campbell, J. Chem. Phys. **79**, 614 (1983).

[6] R. S. Altman, M. D. Marshall, and W. Klemperer, J. Chem. Phys. **77**, 4344 (1982).

[7] (a) C. M. Lovejoy, M. D. Schuder, and D. J. Nesbitt, J. Chem. Phys. **86**, 5337 (1987); (b) G. T. Fraser, A. S. Pine, R. D. Suenram, D. C. Dayton, and R. E. Miller, J. Chem. Phys. **90**, 1330 (1989); (c) D. J. Nesbitt and C. M. Lovejoy, J. Chem. Phys. **96**, 5712 (1992).

[8] R. W. Randall, M. A. Walsh, and B. J. Howard, Faraday Discuss. Chem. Soc. **85**, 1 (1988).

[9] J. K. Rice, R. D. Suenram, F. J. Lovas, G. T. Fraser, and W. J. Lafferty, *Ohio State Symposium on Molecular Spectroscopy*, 1990.

[10] (a) M. A. Walsh, T. H. England, T. R. Dyke, and B. J. Howard, Chem. Phys. Lett. **142**, 265 (1987); (b) K. W. Jucks, Z. S. Huang, D. Dayton, R. E. Miller, and W. J. Lafferty, J. Chem. Phys. **86**, 4341 (1987).

[11] J. Kraitchman, Am. J. Phys. **21**, 17 (1951).

[12] GAUSSIAN 90, M. J. Frisch, , M. Head-Gordon, G. W. Trucks, J. B. Foresman, H. B. Schlegel, K. Raghavachari, M. A. Robb, J. S. Binkley, C. Gonzalez, D. J. Defrees, D. J. Fox, R. A. Whiteside, R. Seeger, C. F. Melius, J. Baker, R. L. Martin, L. R. Kahn, J. J. P. Stewart, S. Topiol, J. A. Pople (Gaussian, Pittsburgh, Pennsylvania, 1990).

[13] S. W. Sharpe, R. Sheeks, C. Wittig, and R. A. Beaudet, Chem. Phys. Lett. **151**, 267 (1988).

[14] J. K. G. Watson, J. Chem. Phys. **46**, 1935 (1967).

[15] C. H. Townes and A. L. Schawlow, *Microwave Spectroscopy* (Dover, New York, 1975), p. 43.

[16] K. K. Leopold, G. T. Fraser, and W. Klemperer, J. Chem. Phys. **80**, 1039 (1984).

[17] Y. P. Zeng, S. W. Sharpe, D. Reifschneider, C. Wittig, and R. A. Beaudet, J. Chem. Phys. **93**, 183 (1990).

[18] M. A. Walsh, T. R. Dyke, and B. J. Howard, J. Mol. Spectrosc. **189**, 111 (1988).

[19] A. C. Legon and A. P. Suckley, J. Chem. Phys. **91**, 4440 (1989).

[20] T. H. Dunning and P. J. Hay, *Methods of Electronic Structure Theory*, edited by H. F. Schaefer III (Plenum, New York, 1977), Chap. 1.

[21] W. R. Wadt and P. J. Hay, J. Chem. Phys. **82**, 284 (1985).

[22] G. Herzberg, *Electronic Spectra and Electronic Structure of Polyatomic Molecules* (Van Nostrand Reinhold, New York, 1966).

[23] G. Herzberg, *Spectra of Diatomic Molecules* (Van Nostrand Reinhold, New York, 1950).

[24] S. F. Boys and F. Bernardi, Mol. Phys. **19**, 553 (1970).

[25] C. C. Costain, J. Chem. Phys. **29**, 864 (1958).

[26] (a) V. W. Laurie and D. R. Herschbach, J. Chem. Phys. **37**, 1687 (1962); (b) W. Gordy and R. L. Cook, *Microwave Molecular Spectra* (Interscience, New York, 1970), Chap. 13.

[27] P. R. Bunker and J. M. R. Stone, J. Mol. Spectrosc. **41**, 310 (1972).

[28] P. R. Bunker and B. M. Landsberg, J. Mol. Spectrosc. **67**, 374 (1977).

[29] P. R. Bunker, Ann. Rev. Phys. Chem. **34**, 59 (1983).

[30] S. Bratoz and M. L. Martin, J. Chem. Phys. **42**, 1051 (1965).

[31] R. J. Le Roy and J. Scott Carley, *Potential Energy Surfaces* (Wiley, New York, 1980), p. 353.

[32] *Dynamics of Polyatomic van der Waals Complexes, NATO ASI Series V. 227*, edited by N. Halberstadt and K. C. Janda (Plenum, New York, 1990).

[33] P. Gröner (private communication).

[34] S. K. Shin, C. Wittig, and W. A. Goddard III, J. Phys. Chem. **95**, 8048 (1991).

[35] G. C. Schatz, M. S. Fitzcharles, and L. B. Harding, Faraday Discuss. Chem. Soc. **84**, 359 (1987).

[36] C. Wittig, Y. M. Engel, and R. D. Levine, Chem. Phys. Lett. **153**, 411 (1988).